International Journal of GEOMATE, Oct., 2024 Vol.27, Issue 122, pp.45-53
ISSN: 2186-2982 (P), 2186-2990 (O), Japan, DOI: https://doi.org/10.21660/2024.122.4549
Geotechnique, Construction Materials and Environment

A NOVEL EMPIRICAL VELOCITY PROFILE OF RIGID SUBMARINE LANDSLIDE-GENERATED TSUNAMI WAVES ON INCLINED PLANES

*Van Khoi Pham[1], Van Nghi Vu[2]

[1]Faculty of Civil Engineering, Vietnam Maritime University, Viet Nam;
[2]Institute of Civil Engineering, Ho Chi Minh City University of Transport, Viet Nam

*Corresponding Author, Received: 10 May 2024, Revised: 20 Aug. 2024, Accepted: 03 Sep. 2024

ABSTRACT: Landslides and landslide-generated tsunami waves arbitrarily happen and cause tremendous hazards to human lives worldwide. Among the recent landslide tsunami events, the rigid submarine landslide sources are becoming more and more concerned due to their mysteries. Dynamical properties of rigid submarine landslides (e.g., velocity) play an important role in the generated tsunami waves. In this study, an empirical velocity profile of rigid submarine landslide-generated waves on an inclined plane is proposed. This new velocity profile is suggested from the velocity profile in a physical experiment of the horizontal rigid submarine landslide-generated waves. A new FLOW-3D HYDRO package is employed to conduct the rigid submarine landslide-generated waves experiment. We first verified the chosen numerical model to the experimental data of rigid submarine landslides moving horizontally. Following the rigid velocity profile on the horizontal plane, we propose a new method to apply it on the inclined plane. The error norm technique is used to find out the empirical velocity profile among 10 critical velocity profiles applied. The novel empirical velocity profile of the critical case of m = 3 as well as critical velocity value of V_c = 0.82 m/s is used to generate tsunami waves, which are in good agreement with the experimental data and better than those of other similar three-dimensional numerical models.

Keywords: Empirical velocity, Rigid body, Submarine landslide, Tsunami wave, FLOW-3D HYDRO.

1. INTRODUCTION

In three recent decades, landslide-induced tsunami waves have become the favored topics of many hydrodynamical researchers [1-6]. Because of the interesting inter-connected phenomena, researchers have been trying to assume the solid kinematics of landslide motions in time and spaces varying water depth [3, 7] as the water wave sources. Compared to the subaerial landslide sources, the submarine landslide sources are more difficult to predict due to their unknown initial properties. In landslide-induced tsunami events [6, 8], the subaerial landslide can reveal the initial volume but the submarine landslide cannot. This leads to tsunami wave heights unpredictable. In addition, the rigid landslide may transfer energy to water waves larger than the deformable landslide [9, 10]. Therefore, it is important to study the rigid submarine landslides-induced tsunami waves.

In rigid submarine landslide-generated tsunami waves, researchers often focus on both physical experiments [1, 11] and numerical experiments [4-5, 12-13]. Thanks to the advantages of numerical experiments, the researchers try to investigate three-dimensional models [4-5, 12-13] as well as two-dimensional models [3, 14]. Three-dimensional models are useful due to no limitations of nonlinearity as well as dispersion at any depth areas compared to other depth-averaged or two-dimensional models [15]. This study also uses the FLOW-3D HYDRO model [16], which solves the fully nonlinear dispersive three-dimensional Navier-Stokes equations, as a tool to investigate the rigid submarine landslide-generated tsunami waves. The previous FLOW-3D model was used to verify the TSUNAMI 3D model and then accurated the spatial-time resolution of deformable subaerial landslide generated tsunami [17, 18] and the diffusion technique of deformable submarine landslide surface-induced tsunami [19]. Until the year of 2021, the new FLOW-3D HYDRO package was developed and then applied to simulate the rigid submarine landslide-induced tsunami waves [13]. However, this study only aimed to validate the numerical model using the physical experiment in [11] and investigate the kinematic effect of rigid submarine landslides (e.g. volume) on generating water wave properties. Until now, the dynamic effect of rigid submarine landslides (e.g., velocity) has not been considered on generating the water waves yet.

Rigid submarine landslides often occur at steep slopes, i.e. 45 degrees [1, 20], due to earthquakes or other seismic phenomena. When moving on the slopes, gravity controls the freely unpredicted motion of those rigid submarine landslides. Thus, in the rigid landslide study, researchers only investigated either landslide mass or slope angle. The rigid landslide motion became the first limitation in the rigid landslide-induced water wave topic. The second limitation was that the wave properties in the onshore direction could not be measured due to the short

distance [21]. Several authors tried to generate tsunami waves using the horizontal motion of rigid elliptical submarine landslides [21, 22]. They could control the horizontal rigid landslide motion (e.g. landslide velocity) as the desired prescribed landslide even if it was not a real phenomenon. This prescribed velocity of rigid submarine landslide was directly used to validate the analytical solution [23, 24] as well as the numerical models of rigid submarine landslide-generated water waves [25, 26]. For the underwater rigid landslide moving on the inclined plane, Yuk et al. [4] employing the COBRAS 3D model and Abadie et al. [5] employing the THETIS 3D model used the prescribed displacement of the body of the experiment of Heinrich [1] in their 3D models to simulate water waves. Until now, the prescribed velocity of that has not yet been used to generate tsunami waves. Thus, the aim of this study is to utilize the prescribed velocity of underwater body movements on a flat bed and apply it to an inclined plane. This modified velocity will provide a new approach to accurately simulate tsunami waves induced by rigid submarine landslides. The FLOW-3D HYDRO model, which has advantages in solving fully dispersive nonlinear phenomena such as landslide-induced tsunami, is employed in this study.

2. MODEL DESCRIPTION

In this section, the water wave module and the rigid body general moving object (GMO) model are introduced to clearly understand the strength of the FLOW-3D HYDRO model [16].

The water wave module applies the framework of Navier-Stokes equations. The continuity and momentum equations [5] are given by

$$\nabla \cdot \left(A\mathbf{u} \right) = 0 \qquad (1)$$

$$\frac{\partial \mathbf{u}}{\partial t} + \frac{1}{V_F}\nabla \cdot (A\mathbf{u}\mathbf{u}) = -\frac{1}{\rho}\nabla \cdot p + G + f_v \qquad (2)$$

where $\nabla = \left(\partial/\partial x, \partial/\partial y, \partial/\partial z \right)$ is the gradient operator, A is the area fraction for the water in the mesh of a Cartesian coordinate system and V_F is the volume fraction for water, $\mathbf{u} = \left(u, v, w \right)$ is the flow velocity in the *x*-, *y*-, *z*-direction; *t* is the time-dependence variable; ρ is the water density; p is the pressure; G is the body acceleration; f_v is the viscous acceleration.

By using the famous volume of fluid (VOF) method [27, 28], the free surface transportation equation between water and air is defined as

$$\frac{\partial V_w}{\partial t} + \frac{1}{V_F}\nabla \cdot \left(V_w A\mathbf{u} \right) = 0 \qquad (3)$$

where V_w is the water volume fraction in the cell of a free surface and $V_w = 0$, $0 < V_w < 1$ and $V_w = 1$ control the different phases of air, interface, and water, respectively.

The turbulence model is applied for solving the dynamic viscosity μ using $k-\varepsilon$, giving the two equations [4] as

$$\frac{\partial k}{\partial t} + \frac{1}{V_F}\left(uA_x\frac{\partial k}{\partial x} + vA_y\frac{\partial k}{\partial y} + wA_z\frac{\partial k}{\partial z} \right) = P_T + G_T + D_k - \varepsilon \qquad (4)$$

$$\frac{\partial \varepsilon}{\partial t} + \frac{1}{V_F}\left(uA_x\frac{\partial \varepsilon}{\partial x} + vA_y\frac{\partial \varepsilon}{\partial y} + wA_z\frac{\partial \varepsilon}{\partial z} \right) = \frac{C_{1\varepsilon}\varepsilon}{k}\left(P_T + C_{3\varepsilon}G_T \right) + D_\varepsilon - C_{2\varepsilon}\frac{\varepsilon^2}{k} \qquad (5)$$

where P_T is the turbulent kinematic energy production; G_T is the buoyancy production term; D_k and D_ε are the diffusion terms; and $C_{1\varepsilon}$, $C_{2\varepsilon}$, $C_{3\varepsilon}$ are constants.

The GMO model describes a rigid body moving in the domain using the motion equation [5] as follows:

$$\mathbf{x}_s = \left[\mathrm{R} \right] \cdot \mathbf{x}_b + \mathbf{x}_G \qquad (6)$$

where $\mathbf{x}_s$ and $\mathbf{x}_b$ are the position vectors of a point in space and body system, respectively, $\mathbf{x}_G$ is the position vector of mass center in space system, and $\left[\mathrm{R} \right]$ is an orthogonal coordinate transformation tensor. Using those position vectors, the rigid body movement properties (e.g. velocity) can be determined in the model.

3. MODEL VERIFICATIONS

In this section, the present simulations of the FLOW-3D HYDRO model are verified using the experimental data in [21, 27], which were recently used to validate the analytical and other numerical models [25, 26]. This experiment showed the underwater rigid elliptic body moving in the horizontal plane as shown in Fig. 1.

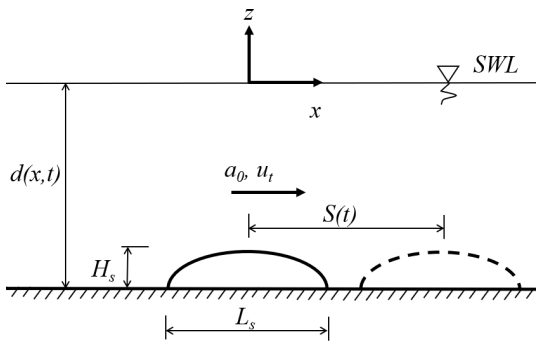

Fig. 1 Schematic of underwater rigid elliptic body in a horizontal plane.

In Fig. 1, the underwater rigid elliptic body had a constant shape with the length of L_s and the height of

H_s, while the water depth $d(x, t)$ changed in space and time when the body moved. It caused the water response at the still water level (*SWL*), and the tsunami waves generally occurred.

In the physical experiment, two rigid body parameters H_s, L_s were fixed, and three parameters a_0, u_t, and d_0 were changed. Where a_0 was the rigid body acceleration, u_t was the rigid body terminal velocity and d_0 was the constant water depth without rigid body height influence. The value of a_0 represented the property of rigid body motion, and the value of u_t represented the strength of rigid body motion. Then, Whittaker et al. [21] grouped those changed values into three dimensionless parameters as follows:

$$\lambda = \frac{a_0}{g}, \quad Fr = \frac{u_t}{\sqrt{g d_0}}, \quad \mu = \frac{d_0}{L_s} \tag{7}$$

where λ was the dimensionless landslide acceleration, Fr was the Froude number and μ was the ratio between the water depth and the landslide length (dispersion parameter). In Eq. (7), the two first parameters represented the rigid body motion and the last parameter represented the dispersion property of the water wave mechanics. Finally, g is the gravitational acceleration.

In this numerical experiment, the water depth changing in space and time [26] is defined as follows:

$$d(x,t) = d_0 - H_s\left[1 - \left(\frac{2\left(x - S(t)\right)}{L_s}\right)^4\right], \quad -\frac{L_s}{2} + S(t) < x < \frac{L_s}{2} + S(t) \tag{8}$$

where $S(t)$ is the rigid body motion, which is described as follows:

$$S(t) = \begin{cases} \frac{1}{2}a_0 t^2, & 0 \le t \le t_1 \\ \frac{1}{2}a_0 t_1^2 + u_t\left(t - t_1\right), & t_1 < t \le t_2 \\ \frac{1}{2}a_0 t_1^2 + u_t\left(t_2 - t_1\right) + u_t\left(t - t_2\right) - \frac{1}{2}a_0\left(t - t_2\right)^2, & t_2 < t \le t_3 \\ \frac{1}{2}a_0 t_1^2 + u_t\left(t_2 - t_1\right) + u_t\left(t_3 - t_2\right) - \frac{1}{2}a_0\left(t_3 - t_2\right)^2, & t > t_3 \end{cases} \tag{9}$$

At each time step, time values are defined as

$$t_1 = \frac{u_t}{a_0}, \quad t_2 = t_1 + 2, \quad t_3 = t_2 + t_1 \tag{10}$$

It means that in the physical experimental mechanism, the velocity accelerates from *0* to u_t in t_1 second. It then maintains a constant value of u_t for *2* seconds before decelerating to *0* in t_1 seconds [21]. This procedure is briefly presented in the velocity profile in Fig. 2.

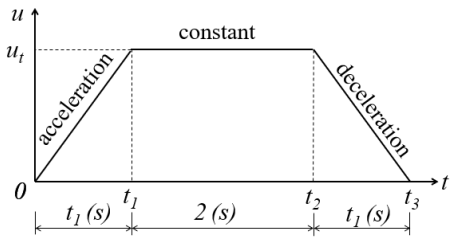

Fig. 2 Underwater rigid elliptic body velocity profile for verification case.

Depending on a_0, u_t and d_0 values, 24 experimental cases were made in [29], but in order to do the numerical verification, only the testing case of run 21 (shown in Table 1) is employed to verify the submarine rigid landslide generated waves using FLOW-3D HYDRO model.

Table 1. Parameters of verification case.

λ	Fr	μ	a_0	d_0	u_t	t_1	t_2	t_3
0.153	0.125	0.35	1.5	0.175	0.164	0.109	2.109	2.218

Note: the unit of t_1, t_2 and t_3 is second, the unit of d_0 is meter, the unit of u_t is m/s, the unit of a_0 is m/s^2.

The experiment was conducted in a flume of length 14.66 m, width 0.25 m and available depth 0.5 m. The rigid elliptic body had a length of L_s = 0.5 m, a width of W_s = 0.25 m, a thickness of H_s = 0.026 m and connected to the mechanical system beneath the flume floor. Finally, the free surface elevations were captured by the laser-induced fluorescence (LIF) technique [21].

In numerical simulations, dimensions of the rigid elliptical body are set to match those of the physical experiment. The domain measures 11.5 m x 0.015 m x 0.22 m with the grid size of 0.005 m, resulting in a total of 303,600 grid cells. This setup ensures accurate wave simulation within the domain while optimizing computational efficiency. The movement of the rigid submarine landslide in the GMO tool is configured using the time and velocity values in Table 1. Boundary conditions are as follows: Z_{min} and Z_{max} are set as wall and air pressure at 101,325 Pa, respectively; X_{min} and X_{max} are set to allow water waves pass through; and Y_{min} and Y_{max} are set to symmetry. Water surface elevations are tracked using VOF technique as mentioned in Eq. (3).

The comparisons between present simulations and experimental data are shown in Fig. 3. Generally, the present simulations show good agreement to the experimental data. The FLOW-3D HYDRO model can accurately simulate the rigid submarine landslide-induced tsunami problem.

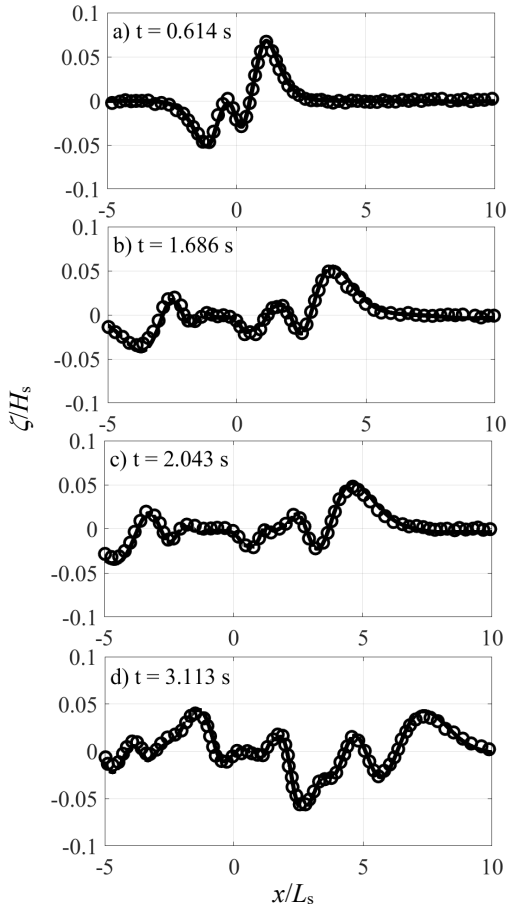

Fig. 3 Verification of present simulations (solid lines) with experimental data (circles) in the test case at a) t = 0.614 s, b) t = 1.686 s, c) t = 2.043 s, d) t = 3.113 s.

In detail, as shown in Fig. 3, the numerical results match the measured data using parameters λ = 0.153, Fr = 0.125 and μ = 0.35 at 4 instant times t = 0.614 s, t = 1.686 s, t = 2.043 s, and t = 3.113 s. In three first instant times, the rigid submarine landslide has not yet stopped (terminal instant time at t_3 = 2.218 s), the water surfaces ζ are not so complicated. After that, at t = 3.113 s, the rigid submarine landslide stops, and then the water surface freely responds in the complicated shape. However, the present simulations can fit all water surface trends.

4. EMPIRICAL VELOCITY PROFILE OF RIGID SUBMARINE LANDSLIDE GENERATED TSUNAMI ON INCLINED PLANES

As mentioned in [21, 27], the landslides moved on the slope subject to gravity control, especially in the buoyancy effect in the submarine landslide case. Then, the velocity profiles of the landslide motions could not be determined exactly as the landslide sources. Therefore, numerical models could only predict approximately the solid submarine landslide-generated tsunami phenomenon [2, 4, 5]. Using the suggestion of the landslide velocity profile in the verification cases, this study proposes an empirical velocity profile appropriate to the application case of the rigid submarine landslide-induced tsunami of Heinrich [1] which was on an inclined plane.

4.1 Laboratory experiment of rigid submarine landslide-induced tsunami on an inclined plane

The physical experiment of rigid submarine landslide-induced tsunami conducted in [1] was used to verify many numerical models [2, 4, 5]. A rigid body, 1 cm underwater, was freely moving down on the first slope of θ = 45°. This body was stopped at the end of the first slope by a buffer as shown in Fig. 4. The first slope had a length of 1 m and a height of 1 m. In this study, to investigate the empirical velocity profile, the second slope is not dealt with here. The rigid body was triangular in shape with dimensions of 0.5 m x 0.5 m and had a density of 2,000 kg/m^3. The water was filled in the height of 1 m and the domain length was 4 m.

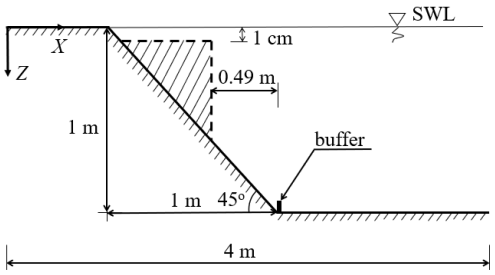

Fig. 4 Schematic of triangular rigid submarine landslide on a steep slope of 45°.

4.2 Empirical velocity profile methodology of rigid submarine landslide moving on inclined planes

This research aims to propose an empirical velocity profile that is appropriate as the freely downslope velocity of the rigid submarine landslide. To obtain this aim, the general velocity profile is assumed and presented in Fig. 5.

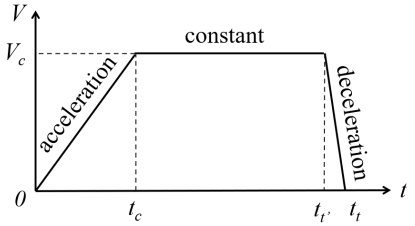

Fig. 5 Empirical velocity profile of the solid motion on inclined planes.

In Fig. 5, V_c is the critical velocity value ($V_c^2 = u_c^2 + w_c^2$). Because the distance in the x dimension is equal to that in the y dimension in this slope of 45°, then the $|u_c|$ value is assumed to be equal the $|w_c|$ value. t_c is the critical time, t_t is the terminal time at the terminal velocity (V_t = 0 m/s at the end of slope), and $t_{t'}$ is the instant time just starting

the decreasing of velocity. Because of the sudden stopping motion of the rigid body by the buffer in this experiment, the author assumes that $t_{t'} \approx t_t = 1$ s.

The proposed acceleration formula of this rigid submarine landslide is given as

$$a(t) = \begin{cases} a_c & if \quad 0 < t \le t_c \\ 0 & if \quad t_c < t \le t_t \end{cases} \quad (11)$$

where a_c is the critical acceleration, and given as follows:

$$a_c = \frac{V_c}{t_c} \quad (12)$$

Then, the velocity formula is given as follows:

$$V(t) = \begin{cases} \frac{V_c}{t_c} t & if \quad 0 < t \le t_c \\ V_c & if \quad t_c < t \le t_t \end{cases} \quad (13)$$

Finally, the rigid submarine landslide moves a distance depending on time as follows:

$$S(t) = \begin{cases} \frac{1}{2}\frac{V_c}{t_c} t^2 & if \quad 0 < t \le t_c \\ \frac{1}{2} V_c t_c + V_c (t - t_c) & if \quad t_c < t \le t_t \end{cases} \quad (14)$$

The proposed rigid velocity profile (Fig. 5) and the rigid motion (Eq. (14)) are similar to those in section 3, which are used to describe the horizontal rigid submarine landslide-induced tsunami problem [21, 26-27].

In Eq. (14), *S(t)* is the distance of the submarine landslide moving on the inclined plane, which can be easily specified at each time step *t*. In the experiment, $S_X(t) = S(t).\cos\theta$ and $S_Z(t) = S(t).\sin\theta$, θ is the slope angle. In order to get two unknown parameters, V_c and t_c, we consider the landslide distance at terminal time $t = t_t = 1$ s. At that time, $S_X(t_t) = S_Z(t_t) = 0.49$ m as shown in Fig. 4.

Then, using Eq. (14), the landslide distance is given as:

$$S(t_t) = V_c (t_t - \frac{1}{2} t_c) \quad (15)$$

Finally, the critical velocity value (in Fig. 5 and Eq. (12-15)) is defined as follows:

$$V_c = \frac{S(t_t)}{(t_t - \frac{1}{2} t_c)} \quad (16)$$

In Eq. (16), only the critical time t_c is the unknown parameter. In this experiment, as the proposed velocity profile shown in Fig. 5, the critical time may have a range from 0 to t_t ($0 < t_c \le t_t$). Subsequently, this study suggests a way to assume the t_c values as shown in the proposal procedure determining V_c values in Fig. 6 as follows:

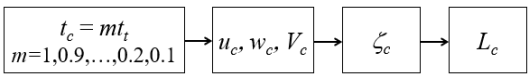

Fig. 6 Proposal procedure determining critical values.

In Fig. 6, the ζ_c is the critical value of rigid vertical displacement/water surface elevation generated by a rigid submarine landslide, which uses the critical velocity values u_c and w_c. The *Lc* is the critical error norm value between rigid vertical displacement/water surface elevation generated by the present model and that of experimental data [1] following Paik [30]. The L_c value shows the sum of the differences between the rigid vertical displacement/water surface elevation along the *x*-direction. In this study, the differences in landslide vertical displacement, L_{cl}, and those of water surface elevations at $t = 0.5$ s, L_{c05}, and $t = 1.0$ s, L_{c10}, are investigated. Whereas, the $\overline{L_c}$ value, which is used to compare the differences among 10 scenarios in numbers, is the average value of L_{c05} and L_{c10}.

4.3 Numerical simulations and empirical velocity value

The FLOW-3D HYDRO is used to simulate the rigid submarine landslide-induced tsunami waves in this study. The computational domain has a length of 4 m, a width of 0.03 m, and a height of 1.1 m, with the grid size of 0.01 m, resulting in a total of 132,000 cells. The water fills the horizontal space from $x = 1$ m to $x = 4$ m and extends to a depth of 1 m, consistent with the physical experiment. The rigid body is triangular in shape (0.5 m x 0.5 m) with a density of 2,000 kg/m^3 and is under a water level of 1 cm. This rigid submarine body is moved under the prescribed motion proposed in subsection 4.2. Boundary conditions are as follows: Z_{min} and X_{min} are set as wall; Z_{max} is set as air pressure at 101,325 Pa; X_{max} is set to allow water waves pass through; and Y_{min} and Y_{max} are set to symmetry.

The results of *m*, t_c, u_c, V_c, ζ_c, L_{cl}, L_{c05}, L_{c10} and $\overline{L_c}$ for 10 scenarios are shown in Table 2. The velocity profiles of V_c for 10 scenarios, which are used for setting up the rigid velocity profiles in this present model, are shown in Fig. 7.

Table 2. The critical parameter results of 10 scenarios.

m	t_c	u_c	V_c	L_{cl}	L_{c05}	L_{c10}	$\overline{L_c}$
1	1	0.98	1.39	0.2379	0.3871	0.4649	0.4260
0.9	0.9	0.89	1.26	0.2312	0.3826	0.4576	0.4201
0.8	0.8	0.82	1.15	0.2068	0.3602	0.4218	0.3910
0.7	0.7	0.75	1.07	0.1837	0.3279	0.3810	0.3545
0.6	0.6	0.70	0.99	0.1412	0.2740	0.3177	0.2959
0.5	0.5	0.65	0.92	0.1012	0.2048	0.2540	0.2294
0.4	0.4	0.61	0.87	0.0508	0.1399	0.2084	0.1742
0.3	**0.3**	**0.58**	**0.82**	**0.0251**	**0.1645**	**0.1631**	**0.1638**
0.2	0.2	0.54	0.77	0.0572	0.1715	0.2111	0.1913
0.1	0.1	0.52	0.73	0.1341	0.2590	0.2455	0.2523

Note: $w_c = u_c$, the unit of t_c is second, the unit of u_c and V_c is m/s.

In Table 2, the minimum value of L_{cl} is 0.0251 and that of $\overline{L_c}$ is 0.1638 corresponding to (L_{c05}, L_{c10}) = (0.1645, 0.1631). Those minimum differences coincidently give the value of m = 0.3, the horizontal-vertical empirical velocity of (u_c, w_c) = (0.58, 0.58) m/s and the total empirical velocity of V_c = 0.82 m/s. Those empirical velocity values and profiles are shown in the thick solid lines when visualized in Fig. 7 and Fig. 8.

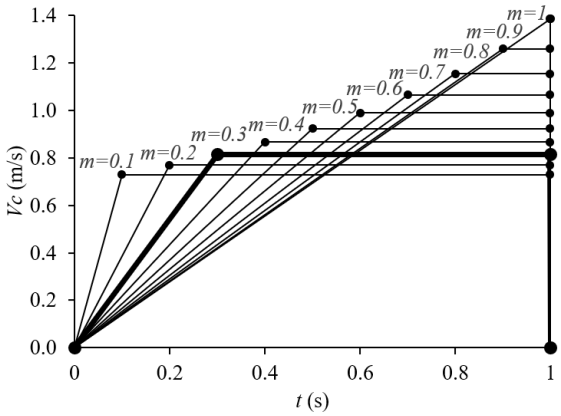

Fig. 7 Empirical velocity profiles of rigid submarine landslide for 10 scenarios.

In Fig. 7, the 10 velocity profiles of 10 scenarios investigated in this study are shown from m = 0.1 to m = 1. Generally, the shapes of those proposed velocity profiles are similar to that of the velocity profile used in the verification cases. However, their shapes are not symmetric in detail. The t_1 value is not equal t_3 value due to the sudden stop of the rigid submarine landslide. Otherwise, the t_2 values decrease and the V_c values increase when the m values increase from 0.1 to 1. These velocity duration and velocity magnitude characteristics of the rigid submarine landslide may affect the generated water waves shown in Fig. 9.

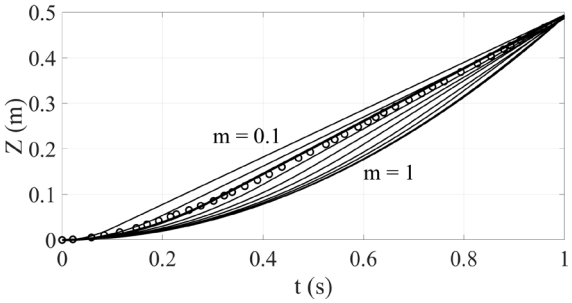

Fig. 8 Comparisons of time-dependent vertical displacement of rigid submarine landslide investigated by present simulations and experimental data in [1] for 10 scenarios.

In Fig. 8, the circle line shows the experimental data of the time-dependent vertical displacement of rigid submarine landslide in the physical experiment in [1]. The solid lines are those in present simulations for 10 scenarios from m = 0.1 to m = 1. As presented in the minimum value of L_{cl}, the empirical case of m = 0.3 gives good agreement to experimental data (the thick solid line in Fig. 8).

Here, to simulate the wave generation, the experimental data at instant times of t = 0.5 s and t = 1.0 s in [1] are chosen to investigate this simulation. The present simulations and the chosen experimental data at t = 0.5 s and t = 1.0 s for 10 scenarios are shown in Fig. 9.

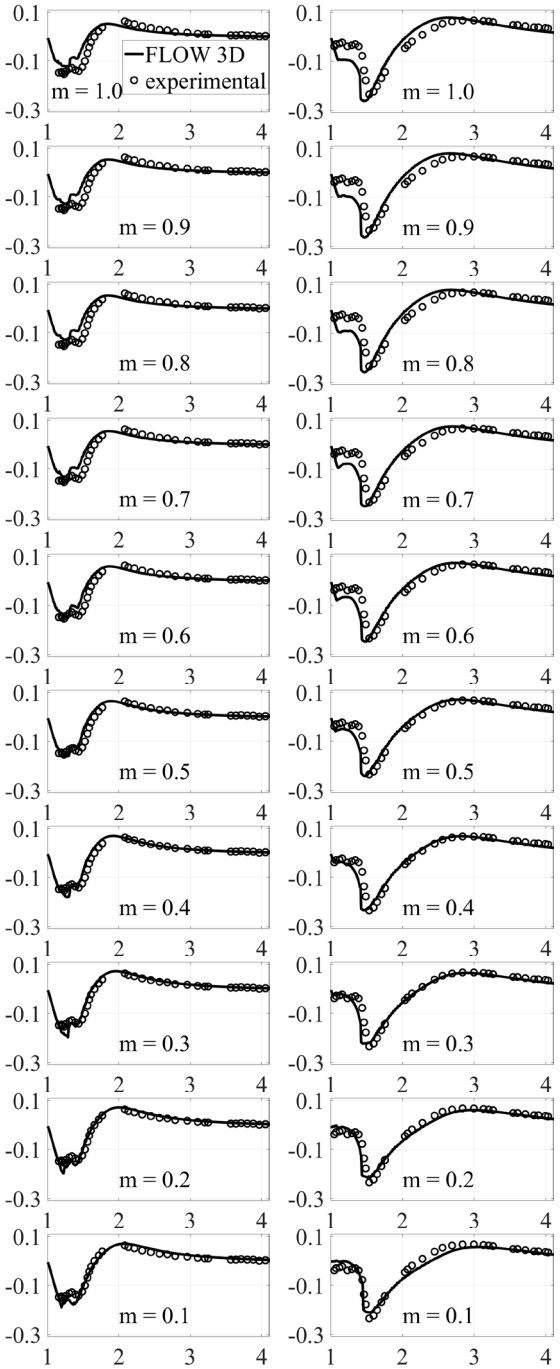

Fig. 9 Comparisons of present simulations (solid line) and experimental data (circle) for 10 scenarios at a) t = 0.5 s (left column), b) t = 1.0 s (right column). Note: the horizontal axis denotes x (m) and the vertical axis denotes ζ (m).

Starting at the case of m = 1.0 in Fig. 7, the velocity profile shows that the acceleration duration is dominated ($t_c \approx 1$ s) and the speed value reaches the largest value (V_c = 1.39 m/s). Those may cause two things in the present simulations at t = 0.5 s and t = 1.0 s. Firstly, the total energy of rigid submarine landslide transfers to water wave too much, thus the wave height at t = 1.0 s is overestimated comparing to the experimental data. Secondly, the energy of rigid submarine landslide transferring to water wave before instant time t = 0.5 s seems to be the smallest, then the wave height is underestimated comparing to the experimental data at t = 0.5 s.

After that, the acceleration duration is decreased, the constant duration is increased and the speed value of the rigid body is decreased. Being explained from the case of m = 0.9 to m = 0.1, the wave heights at instant time t = 1.0 s become gradually underestimated. In comparison, those at instant time t = 0.5 s become gradually overestimated. In this process, it may have the empirical velocity profile where the wave heights of present simulations are fit to those of experimental data. The values of $\overline{L_c}$ in Table 2 present this process in the number values, which decreases from a value of 0.4201 to a minimum value of 0.1638 and increases from a value of 0.1638 to a value of 0.2523. All values indicate the empirical value of m = 0.3 and then the empirical velocity profile is shown by the thick solid line in Fig. 7.

4.4 Comparison to experimental data and other numerical simulations

In this part, the present simulations of water wave surface elevations resulting from the empirical velocity profile are compared to the experimental data [1] as well as other numerical simulations. The chosen numerical models have similar dimensions, governing equations and water surface generation techniques as presented in Table 3. The key problem is only the different rigid submarine landslide tracking methods applied to each model.

Table 3. Statistics of numerical models.

Model	FLOW-3D HYDRO	COBRAS 3D	THETIS 3D
DIM	Three	Three	three
GE	Navier - Stokes	Navier - Stokes	Navier - Stokes
RLT	velocity	displacement	displacement
FST	VOF	VOF	VOF

Note: DIM, GE, RLT and FST denote the dimension, governing equations, rigid landslide tracking and free surface tracking, respectively.

Here, the FLOW-3D HYDRO model is compared to the COBRAS 3D model [4] and the THETIS 3D model [5]. Those numerical simulations and the experimental data at t = 0.5 s and t = 1.0 s are shown in Fig. 10.

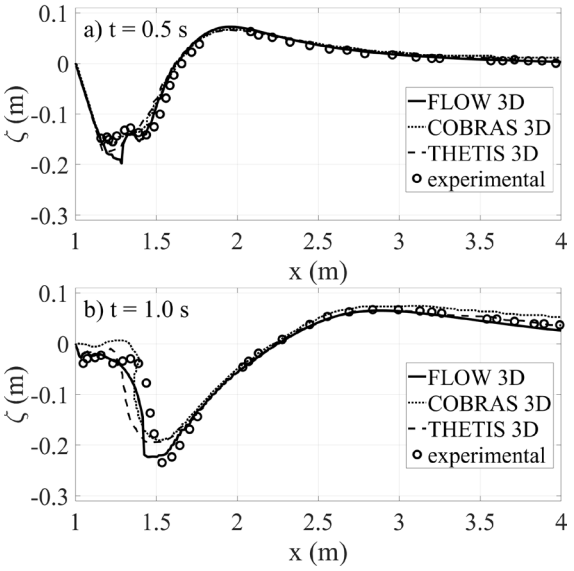

Fig. 10 Comparisons of the present empirical results, COBRAS 3D's simulation [4], THETIS 3D's simulation [5] and experimental data [1] at a) t = 0.5 s, b) t = 1.0 s.

In Fig. 10, the present simulation at t = 0.5 s is not well-fit to the experimental data at locations around x = 1.25 m (see Fig. 10(a)). However, overall comparing to COBRAS 3D's simulation and THETIS 3D's simulation, the present simulation shows better behavior at $x \geq 1.3$ m. In Fig. 10(b), the present simulation generally shows better agreement with experimental data in comparison to COBRAS 3D's simulation and THETIS 3D's simulation. COBRAS 3D's simulation is already overestimated. THETIS 3D's simulation is better than that, but it could not catch the trough of surface elevation. The present simulation is well-fit to both the wave trough and the wave slope around x = 1.5 m, which was a challenge to COBRAS 3D's simulation and THETIS 3D's simulation.

To quantify those agreements, the error norms of those numerical simulations are calculated and shown in Table 4.

Table 4. Comparisons of L error norm of present empirical numerical results and other numerical results to experimental data.

Models	L_{05}	L_{10}	$\overline{L}$
FLOW-3D HYDRO	0.1645	0.1631	**0.1638**
COBRAS 3D	0.2089	0.2458	0.2274
THETIS 3D	0.2071	0.1935	0.2003

The L error norm value at t = 0.5 s of the present simulation is 0.1645, which is the minimum value compared to that of COBRAS 3D's simulation and THETIS 3D's simulation. It is similar to the L error norm value at t = 1.0 s when it gives the minimum value of 0.1631. Thus, the average value of L of this

present simulation is 0.1638, while the L values of COBRAS 3D's simulation and THETIS 3D's simulation are 0.2274 and 0.2003, respectively. Finally, in both qualitative and quantitative, the empirical velocity profile method gives better agreements than others. It is strongly understandable to affirm the right track in the application of this empirical velocity profile.

5. CONCLUSIONS

This study investigates a new empirical velocity profile of rigid submarine landslide-generated tsunami waves using the FLOW-3D HYDRO numerical model. The model is verified against the velocity profile from the physical experiment involving a horizontal rigid submarine landslide of elliptical shape. The verification of the velocity profile for the rigid elliptical source shows good agreements with the resulting water wave elevations comparing to the experimental data. We then modified this velocity profile to discover an empirical velocity profile for a free-slide case of rigid submarine landslide on inclined planes. A procedure process and the error norm technique are employed to determine the empirical velocity profile as well as the critical velocity value over time. In the numerical results, the vertical surfaces of the rigid submarine landslide and the generated water surface elevations are compared to the experimental data in order to identify the critical ones. The empirical velocity profile for the case of $m = 3$ and the critical velocity value of 0.82 m/s of a rigid submarine landslide are used to generate water wave elevations. These are then compared to those generated by other similar 3D models, highlighting the advantages of the novel empirical velocity profile. Although this empirical velocity profile is still bilinear in shape, it can be further developed into a polynomial shape to better fit the rigid submarine landslide surface tracking and the generated water surface elevations.

6. ACKNOWLEDGMENTS

This research is funded by Vietnam Maritime University.

7. REFERENCES

[1] Heinrich P., Nonlinear Water Waves Generated by Submarine and Aerial Landslides, Journal of Waterway, Port, Coastal, and Ocean Engineering, vol. 118, no. 3, 1992, pp. 249–266.

[2] Rzadkiewicz S. A., Mariotti C., and Heinrich P., Numerical Simulation of Submarine Landslides and Their Hydraulic Effects, Journal of Waterway, Port, Coastal, and Ocean Engineering, vol. 123, no. 4, 1997, pp. 149–157.

[3] Lynett P. and Liu P. L.-F., A Numerical Study of Submarine-Landslide-Generated Waves and Run-Up, Proceedings: Mathematical, Physical and Engineering Sciences, vol. 458, no. 2028, 2002, pp. 2885–2910.

[4] Yuk D., Yim S. C., and Liu P. L.-F., Numerical modeling of submarine mass-movement generated waves using RANS model, Computers & Geosciences, vol. 32, no. 7, 2006, pp. 927–935.

[5] Abadie S., Morichon D., Grilli S., and Glockner S., Numerical simulation of waves generated by landslides using a multiple-fluid Navier–Stokes model, Coastal Engineering, vol. 57, no. 9, 2010, pp. 779–794.

[6] Duc D. M., Khang D. Q., Duc D. M., Ngoc D. M., Quynh D. T., Thuy D. T., Giang N. K. H., Van Tien P., Ha N. H., Analysis and modeling of a landslide-induced tsunami-like wave across the Truong river in Quang Nam province, Vietnam, Landslides, vol. 17, no. 10, 2020, pp. 2329–2341.

[7] Watts P., Wavemaker Curves for Tsunamis Generated by Underwater Landslides, Journal of Waterway, Port, Coastal, and Ocean Engineering, vol. 124, no. 3, 1998, pp. 127–137.

[8] Paris A., Heinrich P., Paris R., and Abadie S., The December 22, 2018 Anak Krakatau, Indonesia, Landslide and Tsunami: Preliminary Modeling Results, Pure Appl. Geophys., vol. 177, no. 2, 2020, pp. 571–590.

[9] Ataie-Ashtiani B. and Najafi-Jilani A., Laboratory investigations on impulsive waves caused by underwater landslide, Coastal Engineering, vol. 55, no. 12, 2008, pp. 989–1004.

[10] Yavari-Ramshe S. and Ataie-Ashtiani B., A rigorous finite volume model to simulate subaerial and submarine landslide-generated waves, Landslides, vol. 14, no. 1, 2017, pp. 203–221.

[11] R. Sabeti and M. Heidarzadeh, A new empirical equation for predicting the maximum initial amplitude of submarine landslide-generated waves, Landslides, vol. 19, no. 2, 2022, pp. 491–503.

[12] Ai C., Ma Y., Yuan C., Xie Z., and Dong G., A three-dimensional non-hydrostatic model for tsunami waves generated by submarine landslides, Applied Mathematical Modelling, vol. 96, 2021, pp. 1–19.

[13] Sabeti R. and Heidarzadeh M., Numerical Simulations of Tsunami Wave Generation by Submarine Landslides: Validation and Sensitivity Analysis to Landslide Parameters, J. Waterway, Port, Coastal, Ocean Eng., vol. 148, no. 2, 2022, pp. 491–503.

[14] Dutykh D. and Kalisch H., Boussinesq modeling of surface waves due to underwater landslides, Nonlin. Processes Geophys., vol. 20, no. 3, 2013, pp. 267–285.

[15] Yavari-Ramshe S. and Ataie-Ashtiani B., Numerical modeling of subaerial and submarine landslide-generated tsunami waves—recent

advances and future challenges, Landslides, vol. 13, no. 6, 2016, pp. 1325–1368.
[16] FLOW-3D® Version 2023R1 Users Manual, FLOW-3D [Computer software], Santa Fe, NM: Flow Science, Inc., 2023, pp. 1–164.
[17] Kim G.-B., Numerical simulation of three-dimensional tsunami generation by subaerial landslides, Master's thesis, Civil & Environmental Engineering Dept., Texas A and M Univ., Texas, USA, 2012, pp. 1–89.
[18] Kim G.-B., Cheng W., Sunny R. C., Horrillo J. J., McFall B. C., Mohammed F., Fritz H. M., Beget J., Kowalik Z., Three Dimensional Landslide Generated Tsunamis: Numerical and Physical Model Comparisons, Landslides, vol. 17, no. 5, 2020, pp. 1145–1161.
[19] Horrillo J., Wood A., Kim G.-B., and Parambath A., A simplified 3-D Navier-Stokes numerical model for landslide-tsunami: Application to the Gulf of Mexico: A Simplified 3-D Tsunami Numerical Model, J. Geophys. Res. Oceans, vol. 118, no. 12, 2013, pp. 6934–6950.
[20] Watts P., Tsunami Features of Solid Block Underwater Landslides, J. Waterway, Port, Coastal, Ocean Eng., vol. 126, no. 3, 2000, pp. 144–152.
[21] Whittaker C., Nokes R., and Davidson M., Tsunami forcing by a low Froude number landslide, Environ Fluid Mech, vol. 15, no. 6, 2015, pp. 1215–1239.
[22] Lee S.-J., Yates G. T., and Wu T. Y., Experiments and analyses of upstream-advancing solitary waves generated by moving disturbances, J. Fluid Mech., vol. 199, 1989, pp. 569–593.
[23] Lo H.-Y. and Liu P. L.-F., On the analytical solutions for water waves generated by a prescribed landslide, J. Fluid Mech., vol. 821, 2017, pp. 85–116.
[24] Michele S., Renzi E., A. G. L. Borthwick, C. Whittaker, and A. C. Raby, Weakly nonlinear theory for dispersive waves generated by moving seabed deformation, J. Fluid Mech., vol. 937, 2022, pp. 1–27.
[25] Jing H., Chen G., Liu C., Wang W., and Zuo J., Dispersive effects of water waves generated by submerged landslide, Nat Hazards, vol. 103, no. 2, 2020, pp. 1917–1941.
[26] Tarwidi D., Pudjaprasetya S. R., and Tjandra S. S., A Non-Hydrostatic Model for Simulating Weakly Dispersive Landslide-Generated Waves, Water, vol. 15, no. 4, 2023, pp. 1–13.
[27] Hirt C. W. and Nichols B. D., Volume of fluid (VOF) method for the dynamics of free boundaries, Journal of Computational Physics, vol. 39, no. 1, 1981, pp. 201–225.
[28] Barkhudarov M. R., Lagrangian VOF advection Method for FLOW-3D®, Flow Science Technical Note (FSI-03-TN63), 2004, pp. 1–11.
[29] Whittaker C., Modelling of tsunami generated by the motion of a rigid block along a horizontal boundary, Ph. D. dissertation, University of Canterbury, Christchurch, New Zealand, 2013, pp. 1–357.
[30] Paik J., A high resolution finite volume model for 1D debris flow, Journal of Hydro-environment Research, vol. 9, no. 1, 2015, pp. 145–155.